Journal of Alloys and Compounds 509 (2011) 1172–1177

Contents lists available at ScienceDirect

Journal of Alloys and Compounds

journal homepage: www.elsevier.com/locate/jallcom

Effect of high pressure on photoluminescence properties of Eu^{3+}: K–Ba–Al–fluorophosphate glasses

Ch. Basavapoornima[a], L. Jyothi[a], V. Venkatramu[b], P. Babu[c], C.K. Jayasankar[a,*], Th. Tröster[d], W. Sievers[e], G. Wortmann[e]

[a] Department of Physics, Sri Venkateswara University, Tirupati 517 502, Andhra Pradesh, India
[b] Department of Physics, Yogi Vemana University, Kadapa 516 003, India
[c] Department of Physics, Government Degree and P.G. College, Wanaparthy 509 103, India
[d] Fakultät für Maschinenbau, Universität Paderborn, D-33098 Paderborn, Germany
[e] Department Physik, Universität Paderborn, D-33095 Paderborn, Germany

ARTICLE INFO

Article history:
Received 7 August 2010
Received in revised form
22 September 2010
Accepted 26 September 2010
Available online 28 October 2010

Keywords:
High pressure
Photoluminescence
Eu^{3+} ions
Fluorophosphate glass

ABSTRACT

The effect of hydrostatic pressure and active ion concentration on the luminescence spectra and lifetimes of Eu^{3+}-doped P_2O_5–K_2O–BaO–Al_2O_3–KF glasses have been studied up to 44.8 GPa at room temperature. The $^5D_0 \rightarrow {}^7F_{0-3}$ transitions exhibit pressure induced red-shift with different magnitudes. The crystal-field (CF) strengths at ambient condition are 338, 332 and 350 cm^{-1} for 0.05 mol%, 2.0 mol% and 6.0 mol% Eu_2O_3-doped glasses, respectively. These values slowly increase with increasing pressure and finally reach 518, 410 and 381 cm^{-1} at the highest pressure. The observed increase in the CF strength parameter is found to have an almost cubic dependence on pressure. The luminescence intensity ratio, $^5D_0 \rightarrow {}^7F_2/{}^5D_0 \rightarrow {}^7F_1$, of the Eu^{3+} ions is found to decrease with increasing pressure. The decay curves follow single exponential nature for all the three concentrations of Eu_2O_3-doped glasses for the entire pressure range studied.

1. Introduction

Nowadays, development of optical devices based on rare-earth (RE) ions doped materials is one of the interesting fields of research. Multi-component glasses, which typically consist of network formers and modifiers, provide a wide range of excellent properties and new applications. Moreover, the technological applications of RE luminescence encompass not only fluorescent tubes and colour televisions, but also optical amplifiers and perhaps, very soon organic light emitting diodes.

RE-doped materials have been widely investigated for phosphor and photonic applications. Recent innovations in special photonic glasses and fibers are pushing fiber lasers to the forefront of solid state laser applications and consequently reshaping the laser industry. Glasses doped with RE ions are the material foundation for fiber lasers, upconversion lasers and amplifiers for optical communication. The main goal pursued by many research groups is the optimization of parameters such as emission band width, luminescence lifetime and upconversion efficiency. In this case, parameters such as the cut-off optical phonon energy should be kept small to guarantee low non-radiative losses so that emission could be enhanced. This may be attained by a careful selection of the host constituents.

Efforts have been made on finding materials with low phonon energy in order to reduce the multiphonon non-radiative de-excitation and improve cross-sections of the RE ions, being the fluoride based matrices are the common choices. In this direction, fluorophosphate glasses have received great attention and are the subject of intense research mainly because of their wide transmission range from UV to IR regions and capability of dissolving large amount of foreign ions, such as RE ions without clustering and quenching luminescent properties [1,2]. Recently, researchers focus on the luminescence of RE ions in fluoride glasses, however in fact that the appropriate RE ions can increase fluoride glass stability [2]. Moreover in phosphate glasses, it is difficult to control OH^- group, but it can be possible to minimize the OH^- group in fluorophosphate glasses without protection in special atmosphere [3] and therefore may be considered as active opto electronic materials. Fluorophosphate glass is a suitable optical material with good moisture resistance, physical and chemical stability besides exhibiting significantly reduced non-radiative decay rates between closely spaced RE energy levels due to their low phonon energy. These glasses have low glass transition temperatures and reduced interaction between the dopant and the glass

* Corresponding author. Tel.: +91 877 2248033; fax: +91 877 2225211.
E-mail address: ckjaya@yahoo.com (C.K. Jayasankar).

0925-8388/$ – see front matter © 2010 Elsevier B.V. All rights reserved.
doi:10.1016/j.jallcom.2010.09.167

matrix at the interface. The selection of $Al(PO_3)_3$, $Ba(PO_3)_2$, and KPO_3, as starting materials for phosphate composition has its own advantages compared to other metaphosphates [4]. Here $Al(PO_3)_3$, is added to improve the physical properties of glass. Further addition of fluoride content minimizes OH^- group and hence increases the radiative relaxation of the emitting level.

There are two methods used to understand quantitatively the splitting and shift of the energy levels of lanthanides embedded in solids. The first one is to measure the energy levels of a given lanthanide ion in various host lattices and to study the change in the crystal-field (CF) caused by different environments [5]. The second one is the high pressure technique. The pressure techniques have been used to vary the local environment around active ion sites by tuning inter atomic distances and bond angles [6]. For this, miniature diamond anvil cells (DAC) are used to generate high pressure [7,8]. Pressure dependent luminescence can provide useful information about the interactions between doped ions and the coupling between the dopants and the host.

Among the RE^{3+} ions, Eu^{3+} ion is used as probe due to its simple energy level structure. The luminescence from non-degenerate $^5D_0$ to ^7F_J multiplet gives site symmetry around active ions and number of sites available for active ions. For Eu^{3+} ion, the intense red fluorescence is due to the transitions from the $^5D_0$ level which is lying at much higher energy than that of the next lower level, so the phonon energies of the hosts are not critical to influence the red emission efficiencies. Actually the larger phonon energy can also accelerate the relaxation process, which is beneficial to obtain efficient emission transitions from the $^5D_0$ level [9]. Solid state materials doped with the Eu^{3+} ion have received special interest among the RE activated materials. The Eu^{3+} ion is not only used as a structure probe, but also used in high resolution laser spectroscopy because of the large quadraupole splitting and long spin–lattice relaxation times of its f-electron states. The Eu^{3+} ion is an activator to study the local symmetry as well as CF effect [10–12]. Persistent spectral hole burning can be performed in the $^7F_0 \rightarrow {}^5D_0$ transitions at room temperature. This has potential use in high density optical storage. Also the Eu^{3+} ion has attracted attention in photonic applications because of its red emission from the $^5D_0 \rightarrow {}^7F_2$ transitions.

The spectroscopy of Eu^{3+} ion enables a non destructive diagnostic means of probing the crystallization in the bio-active glass samples which is more sensitive to the small percentage of crystallites [13]. The Eu^{3+} ion luminescence in the yellow-red region is frequently exploited for polychromatic displays. In view of these advantages, the effect of pressure on luminescence properties of Eu^{3+}-doped title glasses has been studied. The effect of a pressure release on these properties has also been studied. CF analysis has been used to evaluate the changes in the local structure around the Eu^{3+} ions under pressure.

2. Experimental details

The Eu^{3+}-doped fluorophosphate glasses with composition (in mol%) of $(56-x/2)\ P_2O_5 + 14\ K_2O + (15-x/2)\ BaO + 6\ KF + 9\ Al_2O_3 + x\ Eu_2O_3$, $x = 0.05$, 2.0 and 6.0 mol% (referred as PKFBAEu) were prepared by conventional melt quenching technique. About 20 g of the batch composition was thoroughly crushed in an agate mortar and the homogeneous mixture was heated in a platinum crucible in an electric furnace for 45 min at a temperature of 1075 °C. The melt was poured onto a preheated brass mold at a temperature of 350 °C and annealed at this temperature for about 15 h to remove thermal strains. Then the sample was allowed to cool to room temperature (RT) and polished for optical measurements.

The fluorescence spectra were recorded with a double monochromator equipped with a photomultiplier tube using the 465.8 nm line of Ar^+ laser as an excitation source. The resolution of the double monochromator depends on the wavelength and on the slit width and it was typically set to 2.0 cm^{-1} over the whole range covered. A special miniature DAC was used to generate pressures up to nearly 44.8 GPa at RT. A piece of the PKFBAEu glass was placed together with a ruby pressure sensor in an 80 μm diameter hole of a stainless steel (INCONEL X750) gasket of 200 μm thickness. A mixture of methanol:ethanol:water (16:3:1) was used as pressure transmitting medium. This gasket with the sample and pressure transmitting fluid was then compressed by the two opposed anvils of the DAC. The pressure and the hydrostatic conditions experienced by the sample were determined by the shift and broadening of the ruby R_1 lines [14]. A mechanical chopper in connection with a multi-channel scalar allowed for lifetime measurement in the range from 2 μs to 2 s.

3. Crystal-field analysis

The detailed description of the CF parameterization for RE ions can be found in the literature [15–17]. The basic expressions for the present calculations have been given here. When a free-ion is introduced into a solid, it experiences an inhomogeneous CF produced by the surrounding charge distribution on ligands. The Hamiltonian that represents the CF potential acting on the RE ion can be expressed in Wybourne's notation as [17]:

$$H_{CF} = \sum_{k,q,i} B_q^k C_q^{(k)}(i) \tag{1}$$

where B_q^k are the CF parameters and $C_q^{(k)}$ are the tensor operators. The B_q^k are treated as adjustable parameters, where as the matrix elements of $C_q^{(k)}$ can be calculated exactly. The number of parameters for H_{CF} in Eq. (1) is greatly reduced by the symmetry selection rules for the point symmetry of the free-ion that can lead to a shift and splitting of the energy levels. Thus the above considerations also apply to materials such as glasses where a long range order does not exist [15]. The disordered nature of the glassy matrix presents a major impediment to the interpretation of the spectra. If the J-mixing effects are neglected then the CF splitting of the $^7F_1$ and $^7F_2$ levels of the Eu^{3+} ion will depend only on the even CF parameters of second and fourth rank ($k = 2$ and 4). The $^7F_1$ level will not split in a cubic CF, and it will split into two levels in hexagonal, trigonal or tetragonal CF. An orthorhombic, monoclinic or a triclinic CF will remove all CF levels that can be observed. In view of these points, it is appropriate to assign the spectra in terms of an average local symmetry in which the immediate environments of the ions are assumed to share a degree of short range order common to all, and that the lowering of symmetry below this level in the bulk reflects largely the randomness orientation from one site to the next [16].

In view of these points, the most appropriate symmetry is C_{2v}; in which full splitting of the $^7F_1$ and $^7F_2$ levels is allowed. Hence, in the present case the CF calculations have been performed by assuming C_{2v} symmetry. The CF strength around active ion in any host can be expressed by the scalar CF strength parameter (S) defined as [18–21]:

$$S = \left\{ \frac{1}{3} \sum_k \frac{1}{2k+1} \left(\left| B_q^k \right|^2 + 2 \sum_{q>0} \left| Re\, B_q^k \right|^2 + \left| Im\, B_q^k \right|^2 \right) \right\}^{1/2} \tag{2}$$

The CF strength parameter (N_V), considering only the second and fourth rank CF parameters has been determined using the following equation:

$$N_V = \sqrt{\frac{4\pi}{5}((B_{20}^2 + 2B_{22}^2) + (B_{40}^2 + 2(B_{42}^2 + B_{44}^2)))} \tag{3}$$

4. Results and discussion

The fluorescence spectra of 0.05, 2.0 and 6.0 mol% Eu_2O_3 doped PKFBAEu glass were measured as a function of pressure and are shown in Fig. 1. The $^5D_0 \rightarrow {}^7F_{4,5,6}$ transitions are not observed, as they are very weak and therefore only the $^7F_0$, $^7F_1$ and $^7F_2$ levels are considered in the analysis. The spectra shown in Fig. 1 are normalized to the $^5D_0 \rightarrow {}^7F_2$ transition. The Eu^{3+} ion emission peaks do not change drastically with pressure either in peak positions or in band width. The emission peaks shifted towards lower energy side

Table 1
Observed and calculated energy levels, luminescence intensity ratio ($I_R(2/1)$), lifetimes (τ, μs), crystal-field parameters (B_{20}, B_{22}, B_{40}, B_{42} and B_{44} cm^{-1}), crystal-field strength (N_V, cm^{-1}) and formal negative charge (q) for 2.0 mol% Eu_2O_3-doped PKFBAEu glass (a) under increasing and (b) decreasing pressures.

Pressure		$^7F_1$			$^7F_2$					$I_R(2/1)$	τ	B_{20}	B_{22}	B_{40}	B_{42}	B_{44}	N_V	q
		A_2	B_1	B_2	A_1	A_1	A_2	B_1	B_2									
(a) Increasing pressure																		
0	Obs	311	402	515	899	930	1034	1143	1228	3.644	2576	537	183	−995	−137	856	332	−0.38
	Cal	286	378	465	900	950	1005	1119	1208									
3.4	Obs	288	393	486	920	959	1040	1129	1230	3.042	2527	583	217	−976	−223	801	343	−1.47
	Cal	284	392	482	916	956	1029	1116	1218									
6.3	Obs	287	397	508	933	964	1048	1142	1234	2.860	2513	603	233	−964	−228	823	350	−2.25
	Cal	286	402	492	920	964	1040	1125	1227									
11.2	Obs	291	401	537	942	978	1070	1155	1234	2.596	2192	649	239	−858	−266	835	356	−2.74
	Cal	290	408	511	923	980	1064	1126	1231									
16.5	Obs	280	403	550	947	981	1074	1162	1249	2.586	2122	696	268	−885	−223	836	358	−4.31
	Cal	279	413	518	925	981	1064	1124	1242									
20.5	Obs	281	398	554	949	987	1074	1196	1231	2.783	2129	636	256	−805	−195	949	361	−5.81
	Cal	284	415	508	913	982	1062	1140	1226									
24.3	Obs	270	399	551	940	977	1061	1190	1225	2.470	2055	637	270	−827	−173	958	362	−7.28
	Cal	277	416	505	910	977	1057	1140	1226									
29.3	Obs	230	381	555	925	969	1037	1185	1251	2.370	2068	749	308	−957	−64	993	374	−7.57
	Cal	246	405	508	891	963	1033	1127	1249									
38.7	Obs	207	384	580	940	1026	1116	1179	1292	2.171	1970	969	393	−755	−166	914	402	−7.72
	Cal	224	418	559	911	999	1094	1105	1269									
44.0	Obs	191	393	593	943	987	1081	1189	1279	1.835	1917	937	436	−878	−96	977	410	−7.43
	Cal	209	428	543	907	980	1071	1120	1273									
(b) Decreasing pressure																		
35.2	Obs	210	382	584	937	990	1081	1170	1214	2.223	1911	537	364	−630	−143	952	373	−7.05
	Cal	228	413	525	898	986	1081	1106	1222									
23.1	Obs	244	384	564	943	972	1066	1138	1209	2.693	1995	583	301	−743	−225	798	351	−5.15
	Cal	256	404	516	917	982	1072	1099	1221									
15.4	Obs	260	394	355	956	977	1061	1111	1180	2.805	2080	603	282	−658	−215	649	306	−3.32
	Cal	269	406	508	938	991	1079	1087	1203									
6.7	Obs	263	393	528	952	966	1027	1099	1173	2.988	2156	649	260	−764	−131	604	281	−1.68
	Cal	267	395	482	934	975	1045	1080	1194									
0.9	Obs	281	369	480	915	965	1014	1088	1156	4.169	2236	696	170	−699	−101	705	270	−0.38
	Cal	283	369	460	911	972	1023	1084	1167									

with increasing pressure accompanied by the decrease of emission intensity [22,23]. The $^5D_0 \rightarrow {}^7F_0$ emission transition is forbidden and the transitions $^5D_0 \rightarrow {}^7F_{2,4}$ are electric-dipole allowed, therefore, their amplitudes are sensitive to changes in the polarizability of the ligand and reduction of the local symmetry around the Eu^{3+} ions. On the other hand, $^5D_0 \rightarrow {}^7F_{1,3}$ transitions are magnetic-dipole allowed and are not much sensitive to changes in the crystalline field. Table 1 presents the pressure-induced Stark level energies (relative to ground $^7F_0$ level) of the $^5D_0 \rightarrow {}^7F_1$ and $^5D_0 \rightarrow {}^7F_2$ transitions of Eu^{3+} ions in the 2.0 mol% Eu_2O_3-doped PKFBAEu glass. The

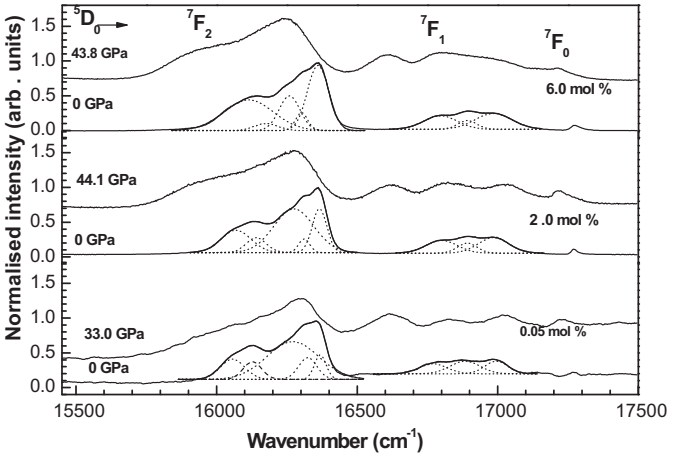

Fig. 1. Luminescence spectra of 0.05, 2.0 and 6.0 mol% Eu_2O_3-doped PKFBAEu glass at different pressures. The spectra are normalized to the maximum intensity of the $^5D_0 \rightarrow {}^7F_2$ transitions. The $^7F_1$ and $^7F_2$ emission peaks are deconvoluted at ambient condition.

values for 0.05 and 6.0 mol% Eu^{3+}-doped glasses follow the similar trend with increase in pressure. There is a progressive broadening for the $^5D_0 \rightarrow {}^7F_{1,2}$ emission bands with increasing pressure. The unique behavior of the longest wavenumber component of the $^5D_0 \rightarrow {}^7F_1$ transition assumes considerable importance, as it is much sharper than the other two components.

Also three components of the $^7F_2$ Stark levels are consistently more intense than the other two. Following the C_{2v} point group correlation, the $^7F_1$ Stark levels belongs to the A_1, B_1 and B_2 representations and the $^7F_2$ Stark levels can be assigned as $2A_1$, A_2, B_1 and B_2 [16]. The $^5D_0 \rightarrow {}^7F_1$ transition has three and the $^5D_0 \rightarrow {}^7F_2$ transition has five Stark splittings which are deconvoluted into three and five Gaussian components as shown in Fig. 1 to give a clear idea about the components of CF levels. Fig. 2 shows the effect of pressure on peak positions of $^5D_0 \rightarrow {}^7F_{0,1,2}$ transitions of 0.05, 2.0 and 6.0 mol% Eu_2O_3-doped glasses. The data points show the experimental data which are fitted to a linear equation to find the shift per GPa (with P in GPa) as [24,25]:

$$E_i(P) = E_i(0) + \alpha_i(P) \quad (4)$$

where i labels one of the four observed transitions. The $E_i(0)$ values of energy positions for the $^5D_0 \rightarrow {}^7F_0$, $^7F_1$, $^7F_2$ and $^7F_3$ bands, respectively, at 0 GPa and the coefficients α_i have been determined from

Table 2
The quantitative red-shifts of $^5D_0 \rightarrow {}^7F_{0,1,2,3}$ multiplets under pressure for different Eu^{3+} ion concentrations in PKFBAEu glasses.

α_i	0.05 mol%	2.0 mol%	6.0 mol%
$\alpha(^5D_0 \rightarrow {}^7F_0)$	−1.6 cm^{-1}/GPa	−1.4 cm^{-1}/GPa	−1.4 cm^{-1}/GPa
$\alpha(^5D_0 \rightarrow {}^7F_1)$	−1.2 cm^{-1}/GPa	−1.6 cm^{-1}/GPa	−3.8 cm^{-1}/GPa
$\alpha(^5D_0 \rightarrow {}^7F_2)$	−1.8 cm^{-1}/GPa	−2.0 cm^{-1}/GPa	−4.3 cm^{-1}/GPa
$\alpha(^5D_0 \rightarrow {}^7F_3)$	–	−1.4 cm^{-1}/GPa	−1.7 cm^{-1}/GPa

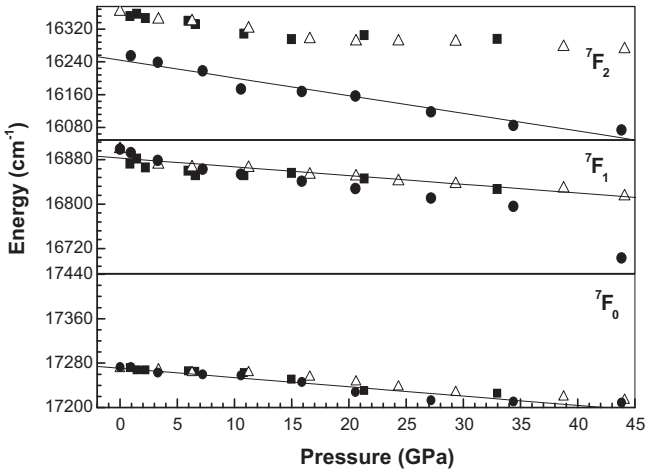

Fig. 2. Peak positions of the $^5D_0 \rightarrow {}^7F_0$, $^7F_1$ and $^7F_2$ transitions of the Eu^{3+} ions in 0.05 (■), 2.0 (△) and 6.0 (●) mol% glasses as a function of increasing pressure. The solid line represents the linear fit to experimental data.

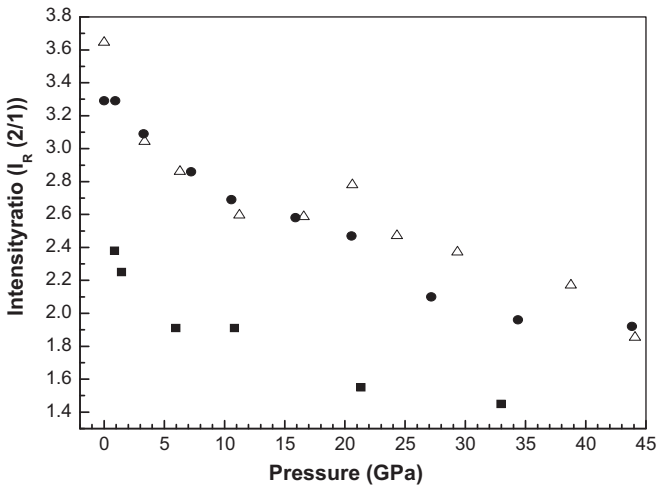

Fig. 3. Luminescence intensity ratio ($I_R(2/1)$) as a function of pressure in 0.05 (■), 2.0 (△) and 6.0 (●) mol% Eu_2O_3-doped PKFBAEu glasses.

the fits. The pressure dependent shifts of the peak positions of Eu^{3+} emission lines found to vary significantly. As shown in Fig. 2, the shift is relatively higher for 6.0 mol% Eu_2O_3-doped glass that could be due to decrease of distance between active Eu^{3+} ions. Pressure induces the increase in the covalency nature for each concentration as evidenced by the values of α_i and formal negative charges (Table 2). The luminescence bands of $^5D_0 \rightarrow {}^7F_{0-2}$ transitions of the Eu^{3+} ions exhibit the red-shift with increasing pressure but with different magnitudes for different concentrations of Eu^{3+} ions. For instance, the shift of the LS manifolds with respect to each other is due to variations in the Coulomb interactions (F^2, F^4 and F^6) and spin–orbit coupling constant, ξ_{4f}. For a given LSJ value, the shift of the Stark levels with respect to each other arises from the variations in the strength and symmetry of the CF acting on the Eu^{3+} ion. Thus, the measured shift of each energy level with pressure can provide the data necessary to probe the Coulomb interaction, the 4f wave functions and/or the CF around the Eu^{3+} ion [26]. The coefficient α_i is higher for 6.0 mol% Eu_2O_3-doped glass for the $^5D_0 \rightarrow {}^7F_2$ transition. This indicates emission of high concentrated active ions doped glass is very sensitive to the pressure and induces relatively higher covalence of Eu^{3+}-ligand bond than in low doped glass.

Inhomogeneous broadening is generally regarded as arising from random processes. The $^5D_0 \rightarrow {}^7F_0$ emission transition between $J = 0$ states has no internal structure and its homogeneous linewidth gives a measure of the energy distribution of the different Eu^{3+} ion sites [27]. Lowering of inversion symmetry leads to a mixing of different parity states, thus allowing electric-dipole transition. Therefore, the amplitudes of electric dipole transitions with respect to magnetic-dipole transitions give a measure of the distortion at the Eu^{3+} sites. Fig. 3 reports the peak intensity ratios $^5D_0 \rightarrow {}^7F_2/{}^5D_0 \rightarrow {}^7F_1$ ($I_R(2/1)$) as a function of pressure. The factor $I_R(2/1)$ is less than one in symmetric and greater than one in non centro symmetric surroundings. From Fig. 3, it is clear that the symmetry is found to be relatively higher in 0.05 mol% Eu_2O_3-doped glass than 2.0 mol% and 6.0 mol% Eu_2O_3-doped glasses, and the $I_R(2/1)$ values are almost similar for 2.0 mol% and 6.0 mol% Eu_2O_3-doped glasses indicating that the distortion of Eu^{3+} sites are minimal. The value of $I_R(2/1)$ decreases with increase in crystallinity but still its value being more than unity suggesting that the Eu^{3+} ions take the accentric sites. Also, this kind of pressure induced reduction in the value of $I_R(2/1)$ has been noticed for amorphous $Eu(OH_3)$ [26], phosphate (PKBAEu) [28] and tellurite (TKNEu10) glasses [29]. By comparing the values of $I_R(2/1)$, it is noted that the intensity ratio is higher for tellurite glasses, intermediate for phosphate glasses and smaller for fluorophosphate glasses. This indicates that the distortion of Eu^{3+} sites is higher in tellurite glasses compared to phosphate and fluorophosphate glasses due to its high covalence. For the PKFBAEu glass the values of $I_R(2/1)$ are 2.25, 3.64 and 3.29 for 0.05, 2.0 and 6.0 mol% Eu_2O_3 concentration, respectively, before pressure is applied and 1.78, 4.16 and 4.36 for 0.05, 2.0 and 6.0 mol% Eu_2O_3 concentration, respectively, when pressure is released after reaching 44 GPa. This indicates that the asymmetry around the Eu^{3+} ions is higher after releasing the pressure than before the pressure is applied. These observations indicate the pressure-induced local deformation at the Eu^{3+} ion sites.

The disordered structure in the glass causes site to site variations. Glasses have a wide variety of environments which can accommodate RE ions in these matrices and therefore the CF effects may change drastically from one site to another. Thus the change in the relative intensities of the optical transitions, the relations between different CF parameters and the CF strength parameter are proposed as the main features to compare and analyze the local environments in different glasses. The CF parameters are products of a pure lattice-dependent factor and ion-dependent 4f-radial integrals. The degeneracy of the $^7F_1$ and $^7F_2$ levels has been completely removed. Thus the local environment occupied by the Eu^{3+} ion in these glasses is assumed as C_{2v}, orthorhombic or triclinic symmetry. The second and fourth rank even CF parameters are calculated by diagonalizing the complete Hamiltonian using C_{2v} symmetry. The fitting process minimizes the root mean square deviation between the experimental and calculated $^7F_1$ and $^7F_2$ Stark energy levels. During the energy level fits, all the 19 free ion parameters ($F^{2,4,6}$, ξ, α, β, γ, $T^{2,3,4,6,7,8}$, $M^{0,2,4}$ and $P^{2,4,6}$) were held fixed to those values of the well know matrix Eu^{3+}: $LaCl_3$ [30]. The effect of pressure on the second and fourth rank CF parameters and on the CF strength parameter N_V is shown in Table 1 for 2.0 mol% Eu_2O_3 doped glass and in Fig. 4. For 0.05 mol% Eu_2O_3-doped glass the CF strength at 6.0 GPa is 358 which is equal to the CF strength at 15.0 GPa in 2.0 mol% and at 6.3 GPa in 6.0 mol% Eu_2O_3-doped glasses. The CF strength N_V increases with increasing pressure. This means that the increase in pressure leads to the decrease in Eu–O inter nuclear distances and also increase in charge density. The variation of fourth rank CF parameters as well as N_V, with good statistical accuracy are found to be a linearly dependent on pressure.

Both the $^5D_0$ and $^7F_0$ levels are immune to ligand field splittings and minor changes in the Eu^{3+} ion environment which are not expected to influence the spin–orbit coupling constant to a

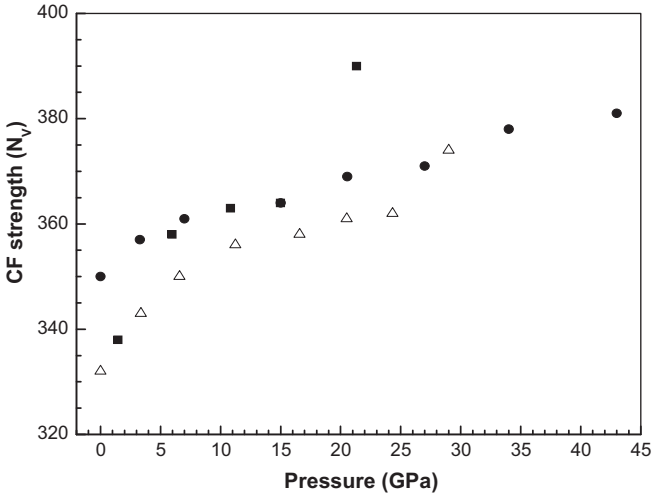

Fig. 4. Variation of crystal-field strength parameter (N_V) with pressure for 0.05 (■), 2.0 (△) and 6.0 (●) mol% Eu_2O_3-doped PKFBAEu glasses.

measurable degree, and hence the observed shifts in $^5D_0 \rightarrow {}^7F_0$ transition energies are attributed to the nephelauxetic effect. That is, the parameters describing interelectronic repulsions in Eu^{3+} ion decrease very slightly as the negative charge on the ligands bonded to Eu^{3+} ion is increased, thus decreasing the energy separation between the $^5D_0$ and $^7F_0$. This formal negative charge (q) can be calculated by using a relationship given by Albin and Horrocks [31]:

$$\nu(\mathrm{cm}^{-1}) = 17273 + 2.29q - 0.76q^2 \quad (5)$$

where q is the total charge (e units) on the ligands and ν is the $^5D_0 \rightarrow {}^7F_0$ transition energy in cm^{-1}. The increase in the value of the formal negative charge on the co-ordinating ligands is a result of the partial transfer of valence electrons. This expansion decreases the electro-negativity of the Eu^{3+} ion and causes an increase in the covalency of the Eu–O bonds as evidenced by the red-shift of the $^5D_0 \rightarrow {}^7F_{0-3}$ transitions under pressure (Table 2). It is now generally attributed that the electro-negativity should be considered as an orbital property rather than atomic property. It is also recognized that the electro-negativity of an orbital is a function of the electron occupancy of that orbital [32]. Therefore, the expansion of the 4f-orbitals of Eu^{3+} ion with the application of pressure decreases concomitantly the electro-negativity of Eu^{3+} ion. Fig. 5 shows the variation of formal negative charge for entire pressure range. The q values are found to be lower in 0.05 mol% doped glass compared to 2.0 and 6.0 mol% Eu^{3+}-doped PKFBAEu glasses.

Fig. 6 shows the variation of formal negative charge with pressure in different hosts [22,28,29]. As can be seen, Eu^{3+}-doped tellurite [29] glass has higher values of formal negative charge compared to all other hosts. The increase in the value of the formal negative charge on the neighboring oxygens can be related to the expansion of f-orbitals of Eu^{3+} ion. This expansion decreases the electro-negativity of the Eu^{3+} ion and causes an increase in the covalency. Therefore, tellurite glasses [29] have higher covalent nature and lithium borate [22] has lower covalence while it is intermediate for phosphate [28] and fluorophosphate glasses.

Fig. 7 shows the decay profiles of the $^5D_0$ level for three Eu^{3+} ion concentrations at different pressures. All the decay curves are single exponential indicating the absence of additional energy transfer processes between Eu^{3+} ions under pressure. The pressure dependence of the lifetime of the $^5D_0$ level of Eu^{3+} ions for 0.05 mol%, 2.0 mol% and 6.0 mol% Eu_2O_3-doped glasses are shown in Fig. 8. As can be seen, the lifetime of the $^5D_0$ level decreases with increasing pressure. Lifetime at ambient pressure is found to be higher for 2.0 mol% (2576 μs) glass compared to 0.05 (2433 μs) and 6.0

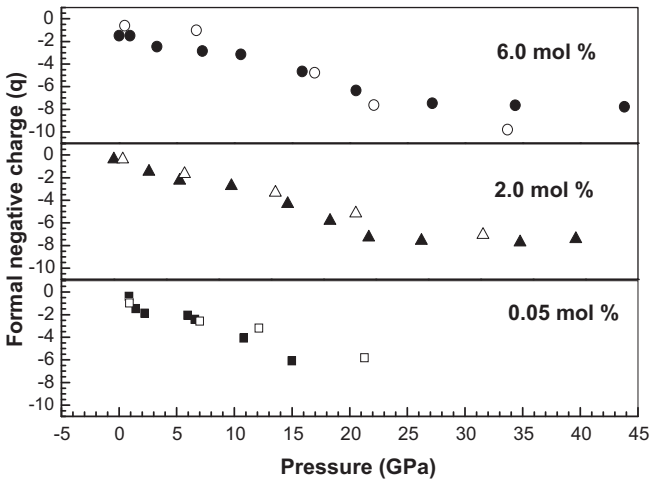

Fig. 5. The variation of formal negative charge (q) on the ligands directly bonded to the Eu^{3+} ion with pressure for 0.05 (■), 2.0 (▲) and 6.0 (●) mol% of Eu_2O_3-doped PKFBAEu glasses. The solid data points refer increasing pressure and the open data points refer decreasing pressure.

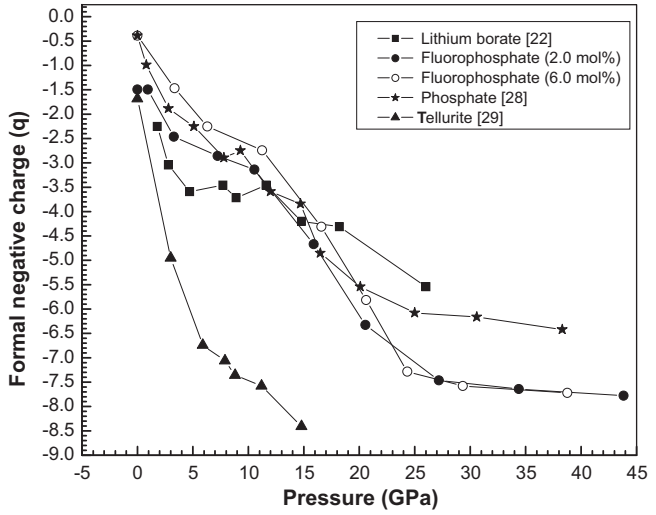

Fig. 6. The variation of formal negative charges with pressure for different Eu^{3+}-doped glasses.

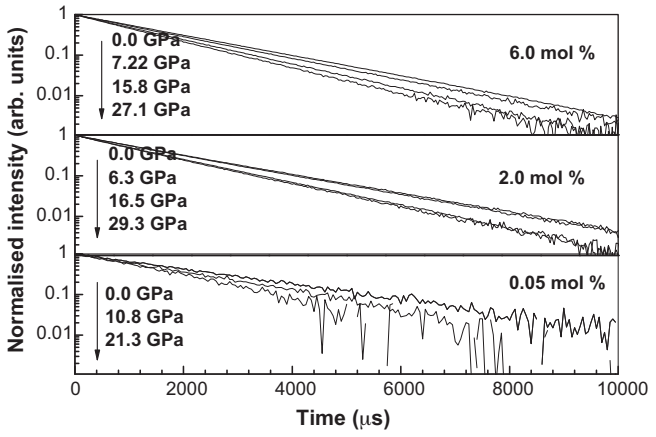

Fig. 7. Decay profiles for the $^5D_0$ level of Eu^{3+} ions in 0.05 mol%, 2.0 mol% and 6.0 mol% Eu_2O_3-doped PKFBAEu glasses at different pressures (λ_{exe} = 465.8 nm).

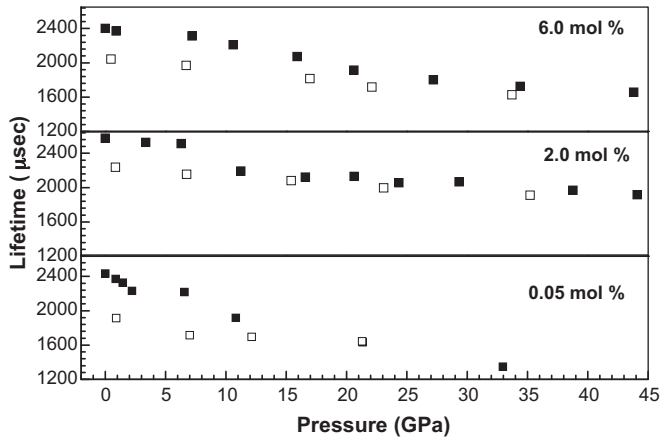

Fig. 8. The variation of lifetime for the $^5D_0$ level of the Eu^{3+} ions in 0.05 mol%, 2.0 mol% and 6.0 mol% Eu_2O_3-doped glasses with pressure. The solid (open) symbol corresponds to data taken at increasing (decreasing) pressure.

(2400 μs) mol% Eu_2O_3-doped glasses. Changes in lifetime may be due to the difference in polarizability of the glass matrices. The shortening of lifetime with increasing pressure is attributed to the gradual increase in energy transfer processes, between Eu^{3+} ions and pressure induced defect centres. A detailed review of such processes was reported by Tröster [15]. In general, either an increase of the multiphonon de-excitation probability or an increase of the electronic transition probability can explain the observed decrease of lifetimes under pressure. The first process can be excluded here because of the large energy gap (12,312 cm^{-1}) between the $^5D_0$ and $^7F_6$ levels, the latter effect is easily explained by the increase in CF strengths around Eu^{3+} ions with pressure. The ambient lifetimes in PKFBAEu glasses are also found to be higher than that of lithium fluoroborate (2039 μs) [22] and tellurite (741 μs) [29] glasses. This may be due to the lower covalence of Eu–O bond in the PKFBAEu glasses.

5. Conclusions

Eu_2O_3-doped K–Ba–Al fluorophosphate glasses with various concentrations were prepared and their concentration and pressure dependent photoluminescence properties have been investigated up to 44.8 GPa. The red-shift of the emission bands with increasing pressure are attributed to the variations of the Coulomb and spin–orbit coupling interactions. The integrated emission intensity ratio, $^5D_0 \rightarrow {}^7F_2/{}^5D_0 \rightarrow {}^7F_1$, of Eu^{3+} ions is found to decrease with increasing pressure indicating the increase in local symmetry around Eu^{3+} ions and the Eu–O covalence which is also evident from the decrease in formal negative charge values with pressure. The local symmetry around the Eu^{3+} ions is higher for lower concentrations (0.05 mol%) of Eu^{3+} ions. The continuous increase in the magnitude of splittings observed for the $^7F_1$ and $^7F_2$ levels with pressure arises from the variations in the strength and symmetry of the crystal-field around the Eu^{3+} ion. The crystal-field strength increases due to charge transfer to the ligands and the creation of high-field Eu^{3+} sites under pressure. The decay curves of the $^5D_0$ level for all the three concentrations remain single exponential for the entire pressure range studied, indicating the absence of additional energy transfer among the active ions. The quenching of lifetimes with increase pressure can be explained by an increase in the electronic transition probabilities and in turn enhancement of CF strength. The pressure induced changes in inter atomic bond length and bond angles are either continuous or discontinuous, as reflected from the pressure induced variation in lifetimes and CF parameters or strengths. The luminescence properties measured at decreasing pressure shows that there is no significant structural hysteresis in the glass matrix.

Acknowledgements

This work has been supported through Major Research Project funded by University Grants Commission (F.32-28/2006(SR) dt. 19-03-2007), Government of India. One of the authors (CKJ) is grateful to Department of Physik, Universität Paderbon, Germany for his stay as a guest scientist.

References

[1] G. Rault, J.L. Adam, F. Smektala, J. Lucas, J. Fluorine Chem. 110 (2001) 165–173.
[2] G. Zhang, M. Poulain, J. Alloys Compd. 275 (1998) 15–20.
[3] M. Liao, Z. Chao Duan, L. Hu, Y. Fang, Leiwen, J. Lumin. 126 (2007) 139–144.
[4] J.H. Campbell, T. Suratwala, J. Non-Cryst. Solids 263 (2000) 318–341.
[5] J. Holsa, P. Porcher, J. Chem. Phys. 76 (1982) 2798–27803.
[6] W. Qiuping, L. Lijun, A.D. Zheng Chiyuanbin, W. Lizhong, J. Phys.: Condens. Matter 4 (1992) 6491–6500.
[7] D.M. Adams, T.K. Tan, J. Phys. Chem. Solids 42 (1981) 559–562.
[8] F. Mamone, M. Nicol, S.K. Sharma, J. Phys. Chem. Solids 42 (1981) 379–384.
[9] H. Lin, D. Yang, G. Liu, T. Ma, B. Zhai, Q. An, J. Yu, X. Wang, X. Liu, E.Y.B. Pun, J. Lumin. 113 (2005) 121–128.
[10] H. Torantani, T. Izumitani, H. Kuroda, J. Non-Cryst. Solids 52 (1982) 303–313.
[11] J.R. Morgan, E.P. Chock, W.D. Hopewell, M.A. Elsayd, R. Orbach, J. Phys. Chem. 85 (1981) 747–751.
[12] S. Tanabe, S. Todoroki, K. Hirao, N. Soga, J. Non-Cryst. Solids 122 (1990) 59–65.
[13] J.K. Krebs, J.M. Brownstein, J. Lumin. 124 (2007) 257–259.
[14] W.B. Holzapfel, J. Appl. Phys. 93 (2003) 1813–1818.
[15] Th. Tröster, in: K.V.A. Gschneidner Jr., J.C.G. Bunzli, V.K. Pecharsky (Eds.), Handbook on the Physics and Chemistry of Rare Earths, vol. 33, Elsevier, Amsterdam, 2003.
[16] C. Brecher, L.A. Riseberg, Phys. Rev. B 13 (1976) 81–93.
[17] B.G. Wybourne, Spectroscopic Properties of Rare Earths, Wiley-Interscience, New York, 1965.
[18] J.A. Capobianco, P.P. Proulx, M. Bettinelli, F. Negrisob, Phy. Rev. B 42 (1990) 5936–5944.
[19] J. Fernandez, R. Balda, J.L. Adam, J. Phys.: Condens. Matter 10 (1998) 4985–5006.
[20] R. Rolli, G. Samoggia, G. Ingletto, M. Bettinelli, A. Speghini, Mater. Res. Bull. 35 (2000) 1227–1234.
[21] M. Zambelli, M. Abril, V. Lavin, A. Speghini, M. Bettinelli, J. Non-Cryst. Solids 345 (2004) 386–390.
[22] C.K. Jayasankar, K. Ramanjaneya Setty, P. Babu, Th. Tröster, W.B. Holzapfel, Phys. Rev. B 69 (2004) 214108–214114.
[23] V. Lavin, P. Babu, C.K. Jayasankar, I.R. Martin, V.D. Rodriguez, J. Chem. Phys. 115 (2001) 10935–10944.
[24] A.G. SouzaFilho, P.T.C. Freire, I. Guedes, F.E.A. Melo, J. MendesFilho, M.C.C. Custodio, R. Lebullenger, A.C. Hernandes, J. Mater. Sci. Lett. 19 (2000) 135–137.
[25] B.R. Jovanic, J. Lumin. 92 (2001) 161–164.
[26] G. Chen, R.G. Haire, J.R. Peterson, High Pressure Res. 6 (1992) 371–377.
[27] R. Campostrini, G. Carturan, M. Ferrari, M. Montagna, O. Pilla, J. Mater. Res. 7 (1992) 745–753.
[28] S. Surendra Babu, P. Babu, C.K. Jayasankar, Th. Tröster, W. Sievers, G. Wortmann, J. Phys.: Condens. Matter 18 (2006) 1927–1938.
[29] R. Praveena, V. Venkatramu, P. Babu, C.K. Jayasankar, Th. Tröster, W. Sievers, G. Wortman, J. Phys.: Conf. Ser. 121 (2008) 042015–042027.
[30] C.K. Jayasankar, F.S. Richardson, M.F. Reid, J. Less-Common Met. 148 (1989) 286–290.
[31] M. Albin, W. Dew Horrocks, Inorg. Chem. 24 (1985) 895–900.
[32] W.L. Jolly, Prin. Inorg. Chem. (1976) 202.